
ON THE APPLICATION OF JAMMALAMADAKA-JIMENEZ GAMERO-MEINTANIS TEST FOR CIRCULAR REGRESSION MODEL ASSESSMENT

A PREPRINT

K. Halaj, B. Klar, B. Milošević, M. Veljović

ABSTRACT

We study a circular-circular multiplicative regression model, characterized by an angular error distribution assumed to be wrapped Cauchy. We propose a specification procedure for this model, focusing on adapting a recently proposed goodness-of-fit test for circular distributions. We derive its limiting properties and study the power performance of the test through extensive simulations, including the adaptation of some other well-known goodness-of-fit tests for this type of data. To emphasize the practical relevance of our methodology, we apply it to several small real-world datasets and wind direction measurements in the Black Forest region of southwestern Germany, demonstrating the power and versatility of the presented approach.

1 Introduction

Circular data has applications in many fields. For example, meteorologists use them to analyze phenomena such as wind direction and ocean currents, ecologists study the direction of animal movement, and economists study calendar effects. However, due to the difference in topology from real-line data, a special methodology is required for such data. A detailed review can be found in [15], including what is done for regression models. Here we focus on the circular-circular regression proposed by [12], defined as follows.

Let Y be a random variable with the density

$$f(y, \delta) = \frac{1}{2\pi} \frac{|1 - |\delta|^2|}{|y - \delta|^2}, \quad y \in \Omega = \{z \in \mathbb{C} : |z| = 1\}, \quad |\delta| \neq 1, \quad (1)$$

where \mathbb{C} is the set of complex numbers and $\delta = e^{i\mu - \gamma}$, for $\mu \in \mathbb{R}$ and $\gamma > 0$. Then we say that Y has the wrapped Cauchy distribution (with mean direction equal to μ) and write $Y \sim WC(\mu, \delta)$. If $\mu = 0$, δ is in $(0, 1)$. If $\delta = 0$, Y has a uniform distribution on the circle, and if δ tends to one, it will be concentrated in the mean direction.

Remark 1 *The random variable Y can be seen as a circular variable since it is a complex number with modulus 1, and is therefore completely defined by the angle in polar representation.*

In [12] the following regression model with wrapped Cauchy errors, was proposed. Let $(x_1, Y_1), \dots, (x_n, Y_n)$ be a sequence of independent circular observations such that

$$Y_i = \beta_0 \frac{x_i + \beta_1}{1 + \beta_1 x_i} \varepsilon_i, \quad x \in \Omega, \quad \varepsilon_i \sim WC(\delta), \quad \text{for some } 0 < \delta < 1, \quad (2)$$

where $\beta_0 \in \Omega$, $\beta_1 \in \mathbb{C}$ and $WC(\delta)$ is short for the wrapped Cauchy $WC(0, \delta)$. Here, β_0 is a rotation parameter; for the interpretation of β_1 , see (author?) [12, p. 635]. $\varepsilon_1, \dots, \varepsilon_n$ are also assumed to be independent.

The main goal of this paper is to provide a powerful diagnostic tool for testing the following assumption about the error distribution:

$$H_0 : \varepsilon_i \sim WC(\delta), \quad \text{for some } \delta \in (0, 1), \quad (3)$$

against the alternative that the errors do not follow a $WC(\delta)$ distribution for any $\delta \in (0, 1)$.

Since the errors $\{\varepsilon_i\}$ are not observable, a natural approach, though not yet used in the context of circular regression models, is to apply the test originally designed for i.i.d. data to model residuals in either complex form or their angular counterparts given by

$$\widehat{\varepsilon}_j = \frac{Y_j}{\widehat{Y}_j}, \quad (4)$$

$$\widehat{\theta}_{\varepsilon_j} = \arg(\widehat{\varepsilon}_j), \quad (5)$$

respectively, and \widehat{Y}_j being the regression estimate (see (6) below). Defining residuals in this way reflects the multiplicative nature of the model. This approach is known as the gold standard for various regression models for linear data types (see, e.g., [6] and [14]). Here we apply goodness-of-fit tests with arbitrary circular distributions proposed in [9] and explore their properties in this setting. The reason for focusing on this statistic, among many proposed for circular data, lies in its dominance over many alternative distributions.

The paper is organized as follows. In Section 2 we present the adaptation of the test statistic from [9]. Its asymptotic properties are discussed in Section 3. The proof of the main result is postponed to the Appendix B. The powers of the test are compared with those of several competitors in Section 4. Section 5 contains several real data examples with small sample sizes and an application to wind direction measurements that clearly illustrate the tests' applicability.

2 Test statistic

As mentioned above, the main idea for testing the hypothesis (3) is to apply tests on the model residuals defined in (4) or (5). Although other estimators could be applied, we follow the original approach of [12] and proceed with the maximum likelihood estimator (MLE) by considering all quantities in (2) in angular form. Let $(x_j, Y_j) = (e^{i\theta_{x_j}}, e^{i\theta_{Y_j}})$ and $(\beta_0, \beta_1) = (e^{i\theta_0}, r e^{i\theta_1})$, where $r > 0, 0 \leq \theta_0, \theta_1 \leq 2\pi$. Then the unknown parameters $v = (\theta_0, \theta_1, r, \delta)$ are obtained by maximizing the log-likelihood function

$$\begin{aligned} \log L(v) &= n \log(1 - \delta^2) \\ &\quad - \sum_{j=1}^n \log(1 - 2\delta \cos(\theta_{y_j} - \theta_0 - \theta_{x_j} + 2 \arg(1 + r e^{i(\theta_{x_j} - \theta_1)})) + \delta^2) + \text{const.} \end{aligned}$$

The estimates are denoted by $\widehat{v} = (\widehat{\theta}_0, \widehat{\theta}_1, \widehat{r}, \widehat{\delta})$. The estimated regression function at $x = x_j$ is then equal to

$$\widehat{Y}_j = \widehat{\beta}_0 \frac{x_j + \widehat{\beta}_1}{1 + \widehat{\beta}_1 x_j} \quad (6)$$

and residuals can be calculated.

The characteristic function of the wrapped Cauchy distribution is given by $\varphi(t, \delta) = \mathbb{E}[e^{it\theta}] = \delta^t$. The empirical characteristic function of the model residuals is given by

$$\varphi_n(t) = \frac{1}{n} \sum_{j=1}^n e^{it\widehat{\theta}_{\varepsilon_j}}.$$

A class of test statistics proposed in [9], modified to test the hypothesis (3), now has the form

$$T_n = n \sum_{t=0}^{\infty} |\varphi_n(t) - \varphi(t, \widehat{\delta})|^2 \omega(t) = n \sum_{t=0}^{\infty} |\varphi_n(t) - \widehat{\delta}^t|^2 \omega(t), \quad (7)$$

where $\omega(\cdot)$ denotes a weight function that satisfies Assumption C from Appendix A. Typically, it is a probability mass function on the non-negative integers with a finite second moment, such as the mass function of the Poisson distribution.

3 Asymptotic properties

Here we present the null distribution of the test statistic T_n under the assumption that the errors in the model follow the wrapped Cauchy distribution with an unknown parameter. For this purpose, following [9], we introduce l_ω^2 - the

separable Hilbert space of all infinite sequences $z = (z_0, z_1, \dots)$ of complex numbers such that $\sum_{t \geq 0} |z_t|^2 \omega(t) < \infty$, where the inner product is defined as $\langle z, u \rangle_\omega = \sum_{t \geq 0} z_t \bar{u}_t \omega(t)$ with $z, u \in l_\omega^2$ and the norm is denoted by $\|\cdot\|_\omega$. With this notation, the test statistic may be written as $T_n = \|G_n\|_\omega^2$, where $G_n(t) = \sqrt{n}(\varphi_n(t) - \varphi(t, \hat{\delta}))$.

Although we assumed in the previous section that all parameters were obtained using the MLE, here we derive the null distribution of T_n under somewhat more general conditions. In particular, we require that Assumptions A, B, and C of the appendix A are satisfied, while it is clear that they are fulfilled for MLE (see, e.g., [8]). We have the following result.

Theorem 1 *If the null hypothesis is true, and under the assumptions A, B, and C given in the Appendix A, there exists a zero-mean Gaussian element $\mathcal{G} \in l_\omega^2$ with covariance kernel $K_{\mathcal{G}}(s, t)$ defined in (9) such that*

$$T_n \xrightarrow{\mathcal{L}} \|\mathcal{G}\|_\omega^2.$$

The proof of the theorem is postponed to the Appendix B. As a corollary, the limiting null distribution of the test statistic T_n can be represented as an infinite weighted sum of independent chi-squared variables. However, these weights are the eigenvalues of the integral operator associated with the kernel $K_{\mathcal{G}}(\cdot, \cdot)$ defined in (9), and computing these eigenvalues is a very difficult task. For more details, we refer to [4]. Therefore, it is recommended to approximate the p -values using bootstrap techniques. For Details, see Appendix D.

4 Empirical study

In this section, we focus on the power performance of T_n with a weight function equal to the probability mass function of the Poisson law with mean $\lambda \in \{0.3, 0.5, 1\}$. The choice of λ follows the results of [9]. For these choices of λ , the probability mass is concentrated on small integer values and down-weights the higher-order terms, which are known to be more susceptible to the periodic behavior inherent in the empirical characteristic function.

We consider the model (2) with $(\beta_0, \beta_1) \in \{(e^{i\frac{\pi}{4}}, 0.9e^{i\frac{\pi}{6}}), (e^{i\frac{\pi}{4}}, 0.1e^{i\frac{\pi}{6}}), (e^{i\frac{3\pi}{4}}, 0.1e^{i\frac{\pi}{6}})\}$. The angles of the covariates $\{\theta_{x_j}, j = 1, \dots, n\}$ in the study are generated from a uniform $U(0, 2\pi)$ distribution.

The idea of applying tests originally for i.i.d. data to model residuals is used here for some other goodness-of-fit tests for circular data. However, we have no results on the validity of these procedures. In particular, we consider

- Kuiper's test with the test statistic

$$K_n = \max_{1 \leq j \leq n} \left\{ U_{(j)} - \frac{j-1}{n} \right\} + \max_{1 \leq j \leq n} \left\{ \frac{j}{n} - U_{(j)} \right\},$$

- Watson's test with test statistic

$$W_n = \frac{1}{12n} + \sum_{j=1}^n \left(\left(U_{(j)} - \frac{2j-1}{2n} \right) - \left(\bar{U} - \frac{1}{2} \right) \right)^2,$$

where $U_{(1)} \leq \dots \leq U_{(n)}$ are the order statistics of $U_j = F(\theta_{\varepsilon_j}, \hat{\delta}), j = 1, \dots, n, \bar{U} = \frac{1}{n} \sum_{j=1}^n U_j$ and $F(\cdot, \delta)$ denotes the distribution function of $WC(\delta)$.

Since the test statistics are not distribution-free, even asymptotically, we approximate their powers and empirical sizes using a warp-speed bootstrap algorithm given in [5] with $B = 10000$ replicates to reduce computing time. We consider the sample sizes $n = 25, 50$ and 100 , and the following alternative distributions for the model innovations:

- wrapped normal ($WN(\rho)$)
- von Mises distribution ($VM(\kappa)$)
- cardioid distribution ($C(\rho)$)
- Cartwright's power-of-cosine distribution ($CW(\zeta)$)
- Jones-Pewsey distribution ($JP(\kappa, \psi)$)
- Batschelet distribution ($Ba(\kappa, \nu)$).

The detailed specification of the alternatives is given in the Appendix C. For all computations in this and the following section, we used the statistical computing environment R [16], together with the R packages `circular` [1] and `cylcop` [7].

Tables 1-3 present the tests' sizes for significance levels $\alpha \in \{0.01, 0.05, 0.1\}$, while Tables 4-6 provide the empirical powers for $\alpha = 0.05$, both evaluated under various model parameters.

We can see that for larger sample sizes all tests are well-calibrated. Considering empirical powers, we can conclude that T_n is more powerful than W_n and K_n , with a tendency for the difference between them to decrease with increasing sample size. It is also important to note the dominance of T_n over close alternatives. When W_n and K_n are compared, W_n is usually more powerful.

		$n = 25$					$n = 50$					$n = 100$				
α	Alternative	$T_n^{(0.3)}$	$T_n^{(0.5)}$	$T_n^{(1)}$	K_n	W_n	$T_n^{(0.3)}$	$T_n^{(0.5)}$	$T_n^{(1)}$	K_n	W_n	$T_n^{(0.3)}$	$T_n^{(0.5)}$	$T_n^{(1)}$	K_n	W_n
0.01	$\mathcal{WC}(0.1)$	1	1	1	1	1	1	1	1	1	1	1	1	1	1	1
	$\mathcal{WC}(0.5)$	1	1	1	1	1	1	1	1	1	1	1	1	1	1	1
	$\mathcal{WC}(0.9)$	1	1	1	1	1	1	1	1	1	1	1	1	1	1	1
0.05	$\mathcal{WC}(0.1)$	4	5	6	5	5	4	5	6	5	5	5	5	5	5	5
	$\mathcal{WC}(0.5)$	5	5	5	4	5	4	4	5	5	5	5	5	5	5	5
	$\mathcal{WC}(0.9)$	6	5	5	5	5	6	6	6	5	5	5	5	5	5	5
0.1	$\mathcal{WC}(0.1)$	9	10	12	10	10	9	10	11	11	10	9	10	10	10	10
	$\mathcal{WC}(0.5)$	10	10	10	10	9	9	9	10	9	9	10	11	11	10	10
	$\mathcal{WC}(0.9)$	11	11	11	10	9	11	11	11	10	10	10	10	10	10	10

Table 1: Empirical sizes for different sample sizes at significance level α ; $\beta_0 = e^{i\frac{\pi}{4}}$, $\beta_1 = 0.9e^{i\frac{\pi}{6}}$

		$n = 25$					$n = 50$					$n = 100$				
α	Alternative	$T_n^{(0.3)}$	$T_n^{(0.5)}$	$T_n^{(1)}$	K_n	W_n	$T_n^{(0.3)}$	$T_n^{(0.5)}$	$T_n^{(1)}$	K_n	W_n	$T_n^{(0.3)}$	$T_n^{(0.5)}$	$T_n^{(1)}$	K_n	W_n
0.01	$\mathcal{WC}(0.1)$	1	1	1	1	1	1	1	1	1	1	1	1	1	1	1
	$\mathcal{WC}(0.5)$	1	1	1	1	1	1	1	1	1	1	1	1	1	1	1
	$\mathcal{WC}(0.9)$	1	1	1	1	1	1	1	1	1	1	1	1	1	1	1
0.05	$\mathcal{WC}(0.1)$	4	5	6	5	5	4	5	5	5	5	4	5	5	5	5
	$\mathcal{WC}(0.5)$	4	5	5	5	5	4	5	5	5	5	5	5	5	5	5
	$\mathcal{WC}(0.9)$	6	6	6	6	5	6	6	6	6	5	6	5	5	5	5
0.1	$\mathcal{WC}(0.1)$	8	10	12	10	10	9	10	12	10	10	8	9	10	10	10
	$\mathcal{WC}(0.5)$	9	9	10	10	9	10	10	10	10	10	10	10	11	11	10
	$\mathcal{WC}(0.9)$	12	12	11	10	10	11	11	11	10	10	11	11	11	10	10

Table 2: Empirical sizes for different sample sizes at significance level α ; $\beta_0 = e^{i\frac{\pi}{4}}$, $\beta_1 = 0.1e^{i\frac{\pi}{6}}$

5 Real data examples

In this section, we fit the circular-circular regression model in (2) to three small datasets from the literature and a larger dataset of wind data from the Black Forest in southwestern Germany and test whether the assumed model is a reasonable choice, i.e. we test the hypothesis in (3). All p -values are obtained using $B = 10000$ bootstrap replicates.

Example 1: The wind direction at 6 a.m. and 12 p.m. was measured every day for 21 consecutive days at a weather station in Milwaukee [11]. The dataset is shown in Table 7. We use model (2) to regress the wind direction at noon to the wind direction at 6 am. The maximum likelihood estimates are $\hat{\theta}_0 = 1.27$, $\hat{r} = 0.53$, $\hat{\theta}_1 = 2.59$, and $\hat{\delta} = 0.55$. The results of the different goodness-of-fit tests shown in the first row of Table 10 indicate that the data are consistent with the model (2).

Example 2: In a medical experiment, several measurements were taken on 10 medical students several times a day over several weeks [3]. The estimated peak times (converted into angles θ and ϕ) for two consecutive measurements

		$n = 25$					$n = 50$					$n = 100$				
α	Alternative	$T_n^{(0.3)}$	$T_n^{(0.5)}$	$T_n^{(1)}$	K_n	W_n	$T_n^{(0.3)}$	$T_n^{(0.5)}$	$T_n^{(1)}$	K_n	W_n	$T_n^{(0.3)}$	$T_n^{(0.5)}$	$T_n^{(1)}$	K_n	W_n
0.01	WC(0.1)	1	1	1	1	1	1	1	1	1	1	1	1	1	1	1
	WC(0.5)	1	1	1	1	1	1	1	1	1	1	1	1	1	1	1
	WC(0.9)	1	1	1	1	1	1	1	1	1	1	1	1	1	1	1
0.05	WC(0.1)	4	5	6	5	4	4	5	6	5	5	4	4	5	5	4
	WC(0.5)	4	4	5	5	5	5	5	5	5	5	5	5	5	5	5
	WC(0.9)	5	5	6	5	5	6	6	6	5	5	5	5	5	5	5
0.1	WC(0.1)	8	9	12	10	9	8	10	11	9	10	8	9	10	10	9
	WC(0.5)	9	9	10	10	9	10	10	10	10	10	10	10	11	10	10
	WC(0.9)	11	11	10	10	10	11	11	11	10	11	11	11	11	10	10

Table 3: Empirical sizes for different sample sizes at significance level α ; $\beta_0 = e^{i\frac{3\pi}{4}}$, $\beta_1 = 0.1e^{i\frac{\pi}{6}}$

		$n = 25$					$n = 50$					$n = 100$				
Alternative	$T_n^{(0.3)}$	$T_n^{(0.5)}$	$T_n^{(1)}$	K_n	W_n	$T_n^{(0.3)}$	$T_n^{(0.5)}$	$T_n^{(1)}$	K_n	W_n	$T_n^{(0.3)}$	$T_n^{(0.5)}$	$T_n^{(1)}$	K_n	W_n	
WN(0.5)	4	5	6	5	5	14	16	18	11	10	45	47	46	30	31	
WN(0.7)	7	7	8	7	6	45	46	45	29	26	92	93	91	72	68	
WN(0.9)	8	8	7	12	10	77	75	70	56	48	97	97	95	87	84	
VM(0.9)	4	5	5	5	4	4	5	5	5	5	8	9	9	7	7	
VM(2)	5	5	5	6	5	25	25	25	18	17	68	68	65	45	45	
VM(5)	7	7	6	12	9	71	68	61	48	43	96	96	94	84	80	
VM(7)	5	6	6	13	11	73	72	69	55	49	96	96	94	87	83	
Ca(0.3)	4	5	7	5	5	5	6	7	5	6	8	9	10	8	7	
Ca(0.5)	6	8	9	6	6	26	29	33	18	17	72	75	75	51	48	
CW(0.5)	8	8	9	8	7	54	55	55	33	29	94	94	94	78	75	
CW(1)	7	8	9	6	6	25	29	33	18	18	72	75	75	51	48	
JP(2,0)	5	5	4	6	5	27	26	25	18	17	67	67	64	45	45	
JP(2,1)	6	7	9	6	6	21	25	28	16	16	63	66	66	43	41	
JP(2,1.5)	4	5	7	6	5	13	16	19	11	10	43	47	49	30	29	
Ba(3,0.5)	4	4	4	8	7	45	45	41	33	30	83	82	78	65	62	
Ba(3,1)	2	3	3	10	8	37	39	39	36	33	77	78	78	68	65	

Table 4: Empirical size (first 3 lines) and power (expressed as a percentage) for different sample sizes at significance level 0.05; $\beta_0 = e^{i\frac{\pi}{4}}$, $\beta_1 = 0.9e^{i\frac{\pi}{6}}$

of diastolic blood pressure are given in Table 8. The estimated parameters are $\hat{\theta}_0 = 0.01$, $\hat{r} = 0.06$, $\hat{\theta}_1 = 5.22$, and $\hat{\delta} = 0.97$. The value of $\hat{\delta}$ is close to 1, indicating that covariates and responses are correlated almost without error. A look at the fitted values confirms this, see the third row in Table 8. As expected, the validity of model (2) is supported by the results of the goodness-of-fit tests given in the second row of Table 10.

Example 3: This data set contains 38 phase or peak expression times of synchronized circadian-related genes common to heart and liver tissue in vivo [13]. The phase angles (in radians) of the circadian-related transcripts in the heart and liver are given in Table 9. The maximum likelihood estimates are $\hat{\theta}_0 = 0.11$, $\hat{r} = 0.27$, $\hat{\theta}_1 = 2.36$, and $\hat{\delta} = 0.61$. Again, the p -values shown in the third row of Table 10 support the validity of the regression model in (2).

Example 4: The wind conditions at a potential site are critical to the design of wind turbines. When considering a site, the local wind conditions are analyzed using calculations based on reference values or on-site measurements. The second method is expensive and only available for relatively short periods. Reference values are usually available free of charge for long periods, but the reference sites are more or less far away and the transferability must be quantified.

We consider datasets from the German Weather Service, available at https://opendata.dwd.de/climate_environment/CDC/observations_germany/climate/hourly/wind/. The accuracy of the wind direction measurement is 10 degrees, so all values are multiples of 10. We use data from two nearby stations in the Black Forest in southwestern Germany, Freudenstadt (fr) and Hornisgrinde (ho), at a distance of about 22 km. We regress the values

Alternative	$n = 25$					$n = 50$					$n = 100$				
	$T_n^{(0.3)}$	$T_n^{(0.5)}$	$T_n^{(1)}$	K_n	W_n	$T_n^{(0.3)}$	$T_n^{(0.5)}$	$T_n^{(1)}$	K_n	W_n	$T_n^{(0.3)}$	$T_n^{(0.5)}$	$T_n^{(1)}$	K_n	W_n
$\mathcal{WN}(0.5)$	5	6	8	7	6	20	22	23	15	15	54	56	55	36	38
$\mathcal{WN}(0.7)$	12	12	13	12	11	54	54	52	37	34	97	97	97	81	77
$\mathcal{WN}(0.9)$	14	14	12	17	15	82	80	76	60	52	100	100	100	99	95
$\mathcal{VM}(0.9)$	3	4	5	4	5	5	6	6	6	6	11	12	12	9	10
$\mathcal{VM}(2)$	7	7	7	8	8	30	29	28	21	21	78	77	75	56	56
$\mathcal{VM}(5)$	12	11	10	16	14	76	74	68	52	47	100	100	100	96	92
$\mathcal{VM}(7)$	9	10	10	16	14	77	77	73	56	49	100	100	100	98	94
Ca(0.3)	4	5	6	5	5	6	7	8	6	7	11	11	12	9	10
Ca(0.5)	8	9	12	8	8	34	37	38	24	24	81	83	82	60	59
CW(0.5)	13	14	16	12	11	62	62	60	40	36	98	99	98	88	83
CW(1)	8	9	12	8	8	34	37	38	24	24	81	83	82	60	59
JP(2,0)	6	6	6	8	8	30	30	29	21	20	77	77	75	55	55
JP(2,1)	7	8	11	8	8	27	30	31	20	20	72	75	75	53	53
JP(2,1.5)	5	7	9	7	7	17	20	21	14	14	53	56	56	39	40
Ba(3,0.5)	7	7	7	12	11	50	49	45	35	31	95	95	94	81	79
Ba(3,1)	4	4	5	12	11	42	42	42	37	32	93	94	94	83	79

Table 5: Empirical powers (expressed as a percentage) for different sample sizes at significance level 0.05; $\beta_0 = e^{i\frac{\pi}{4}}, \beta_1 = 0.1e^{i\frac{\pi}{6}}$

Alternative	$n = 25$					$n = 50$					$n = 100$				
	$T_n^{(0.3)}$	$T_n^{(0.5)}$	$T_n^{(1)}$	K_n	W_n	$T_n^{(0.3)}$	$T_n^{(0.5)}$	$T_n^{(1)}$	K_n	W_n	$T_n^{(0.3)}$	$T_n^{(0.5)}$	$T_n^{(1)}$	K_n	W_n
$\mathcal{WN}(0.5)$	5	7	9	7	7	20	22	23	15	15	54	56	55	37	39
$\mathcal{WN}(0.7)$	12	12	13	13	11	54	53	52	37	34	97	97	97	81	78
$\mathcal{WN}(0.9)$	15	15	12	18	16	82	81	77	60	53	100	100	100	98	95
$\mathcal{VM}(0.9)$	4	4	6	5	5	5	6	7	6	6	11	12	12	10	10
$\mathcal{VM}(2)$	7	7	8	9	9	31	30	29	22	22	78	78	75	56	57
$\mathcal{VM}(5)$	13	13	11	17	15	76	74	68	51	47	100	100	100	96	92
$\mathcal{VM}(7)$	11	12	12	17	15	77	76	73	56	49	100	100	100	98	94
Ca(0.3)	4	4	6	6	5	7	8	9	7	7	11	12	13	9	10
Ca(0.5)	9	11	14	9	9	34	37	38	25	24	80	82	82	60	59
CW(0.5)	14	15	17	13	11	62	62	61	39	36	98	99	98	87	83
CW(1)	9	11	14	9	9	34	37	38	25	24	80	82	82	60	59
JP(2,0)	7	6	7	9	9	30	29	29	21	21	77	77	75	55	55
JP(2,1)	8	9	12	9	9	28	31	32	20	20	72	75	75	53	54
JP(2,1.5)	6	8	11	8	8	19	21	21	14	15	53	56	56	38	39
Ba(3,0.5)	8	7	7	13	12	50	49	46	35	32	95	95	94	82	79
Ba(3,1)	5	5	6	12	11	41	43	43	36	32	93	94	94	83	78

Table 6: Empirical powers (expressed as a percentage) for different sample sizes at significance level 0.05; $\beta_0 = e^{i\frac{3\pi}{4}}, \beta_1 = 0.1e^{i\frac{\pi}{6}}$

6 a.m.	356	97.2	211	232	343	292	157	302	335	302	324
	84.6	324	340	157	238	254	146	232	122	329	
12 a.m.	119	162	221	259	270	28.8	97.2	292	39.6	313	94.2
	45	47	108	221	270	119	248	270	45	23.4	

Table 7: Dataset 1 - Wind direction (in degrees)

at a station as the potential site on the nearby "reference station" as a proxy for what is done in real projects. The datasets contain wind directions measured at 6:00 am and noon on Wednesdays over 9 years, from 2015/01/07 to 2023/12/27. After removing a small number of missing values, the sample size of each measured variable is 463. The

θ	30	15	11	4	348	347	341	333	332	285
ϕ	25	5	349	358	340	347	345	331	329	287
$\hat{\phi}$	24	9	5	359	344	343	337	330	329	287

Table 8: Dataset 2 - Blood pressure

θ	0.12	0.27	0.29	0.3	0.31	0.34	0.35	0.58	0.62	1.6
	2.35	2.62	2.83	-3.06	-2.86	-2.77	-2.69	-2.57	-2.56	-2.45
	-2.43	-2.37	-2.18	-2.16	-2.04	-1.61	-1.32	-1.22	-0.84	-0.77
	-0.38	-0.36	-0.26	-0.19	-0.18	-0.13	-0.12	-0.02		
ϕ	0.61	0.95	-2.85	0.67	-0.13	0.08	2.67	1.72	1.45	1.59
	-2.51	-2.92	1.42	2.74	2.88	-3.01	-2.69	3.05	-2.35	2.68
	-2.86	-2.51	2.69	-2.11	-1.48	-2.06	-2.63	-1.49	-0.83	0.86
	0.26	1.5	1.03	0.33	-1.15	-0.21	-0.55	0.91		

Table 9: Dataset 3 - Peak expression times

Dataset	$T_n^{(0.3)}$	$T_n^{(0.5)}$	$T_n^{(1)}$	K_n	W_n
wind direction	0.18	0.12	0.06	0.39	0.56
blood preasure	0.58	0.59	0.62	0.73	0.70
peak times	0.36	0.33	0.30	0.77	0.77

Table 10: Empirical p -values for data examples in Section 5

four resulting data sets are fr06, fr12, ho06 and ho12. Although the lag between consecutive observations is one week, the data are time series. Therefore, we computed autocorrelations of the four data sets, using a correlation coefficient for angular variables proposed in [10]. The lag-one autocorrelations for the four datasets are 0.093, 0.019, -0.003 and 0.113, and the p -values for corresponding tests of the hypothesis that the autocorrelation is zero are 0.043, 0.686, 0.946 and 0.017. We also computed autocorrelations for lags 2 through 5 (corresponding to 2-5 weeks), which yielded two values between 0.1 and 0.2; the remaining values are below 0.1. Out of a total of 20 tests, only one is significant at the 0.01 level. In summary, the serial correlation within the time series is low and does not invalidate the subsequent analysis. Figure 1 shows stack plots of the wind directions at the two sites.

We now regress the values at the Hornisgrinde station at noon (ho12) on the corresponding values at the Freudenstadt station (fr12), and repeat the same with the data at 06:00.

As further examples, we regress the wind direction at noon on the wind direction at 6 am as in Example 1 in Section 5 to mimic a forecast scenario. The estimated parameters of the 4 regression models are given in Table 11.

The conditional distribution of $Y|x$ in model (2) is a wrapped Cauchy distribution $WC(\mu_{y.x}, \delta_{Y|x})$ with

$$\mu_{y.x} = \arg \left(\beta_0 \frac{x + \beta_1}{1 + \bar{\beta}_1 x} \right), \quad \delta_{Y|x} = \exp(i\mu_{y.x})\delta$$

(see (author?) [12, p. 638]). Thus, the circular variance takes the constant value $1 - \delta$, while the circular mean is $\mu_{y.x}$. The last two columns of Table 11 show as an example the fitted $\hat{\mu}_{y.x}$ for $x = \pi/4$ and $x = 3\pi/4$. Figure 2 shows stack plots of the residuals from the 4 regression models.

The results of the goodness-of-fit tests for the full data sets, using 10000 replications, are shown in the upper panel of Table 12. Due to the length of the dataset, it is not surprising that the first three models have p -values close to zero. However, for the last regression model, the p -values are all above 0.05. In the middle and bottom panel, we have reduced the sample to 200 and 100 observations, roughly corresponding to 2020-23 and 2022-23, respectively. For $n = 200$, the second model is still clearly rejected by all tests, and the p -values for the first model are below 0.05 for all tests except K_n , while the p -values for model 3 are below 0.05 only for the tests based on K_n . For $n = 100$, the p -values are generally higher, and never below 0.03. Again, the p -values for model 4, which regresses fr12 on fr06, are higher than for the other models. All in all, the proposed model seems to be a reasonable model for the application under consideration.

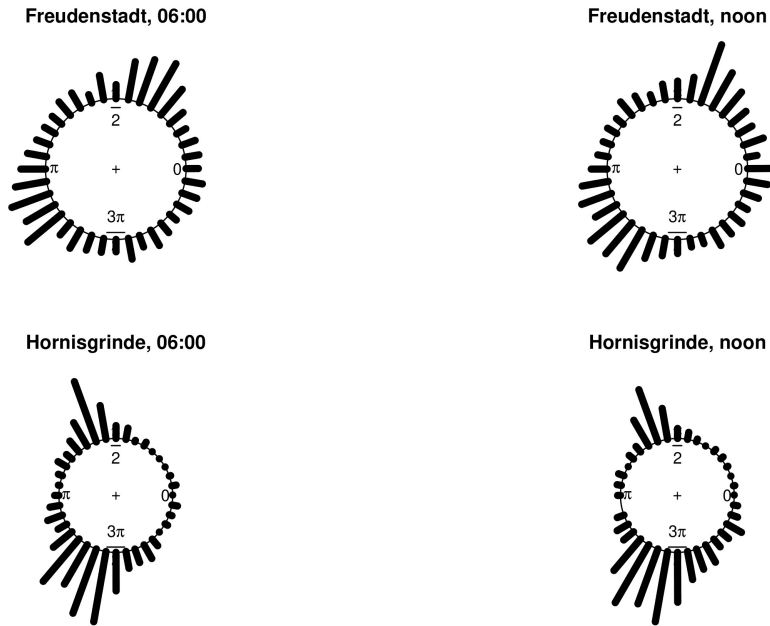


Figure 1: Stack plot of the wind directions at the two sites, measured at 06:00 and noon over 9 years from 2015 to 2023.

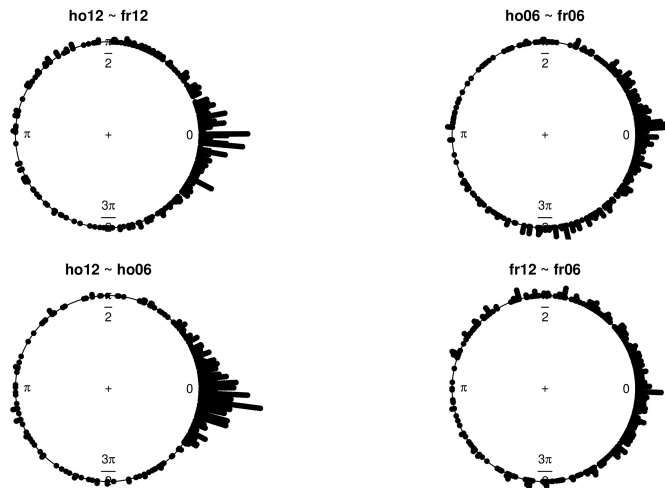


Figure 2: Stack plot of the residuals $\hat{\theta}_\varepsilon$ of the different regression models.

x	y	n	$\hat{\theta}_0$	$\hat{\theta}_1$	r	δ	$\hat{\mu}_{y,\pi/4}$	$\hat{\mu}_{y,3\pi/4}$
fr12	ho12	463	0.59	3.70	0.36	0.65	1.62	3.57
fr06	ho06	463	1.37	2.65	0.51	0.54	3.20	3.93
ho06	ho12	463	6.18	4.79	0.24	0.75	0.25	2.64
fr06	fr12	463	0.28	0.36	0.07	0.45	1.02	2.51

Table 11: Estimated parameters of the different regression models using the Black Forest wind data.

n	x	y	$T_n^{(0.3)}$	$T_n^{(0.5)}$	$T_n^{(1)}$	K_n	W_n
463	fr12	ho12	0.00	0.00	0.00	0.00	0.00
	fr06	ho06	0.00	0.00	0.00	0.00	0.00
	ho06	ho12	0.01	0.01	0.01	0.01	0.04
	fr06	fr12	0.09	0.10	0.11	0.07	0.07
200	fr12	ho12	0.02	0.02	0.04	0.11	0.02
	fr06	ho06	0.00	0.00	0.00	0.00	0.00
	ho06	ho12	0.26	0.23	0.18	0.01	0.08
	fr06	fr12	0.11	0.12	0.16	0.31	0.23
100	fr12	ho12	0.04	0.04	0.04	0.14	0.22
	fr06	ho06	0.03	0.03	0.03	0.10	0.27
	ho06	ho12	0.49	0.37	0.23	0.16	0.29
	fr06	fr12	0.98	0.98	0.97	0.93	0.91

Table 12: Empirical p -values for the different regression models using the Black Forest wind data.

Acknowledgements

The research was done as a part of the bilateral cooperation project Modeling complex data - Selection and Specification between the Federal Republic of Germany and the Republic of Serbia funded by the Federal Ministry of Education and Research of Germany and the Ministry of Science, Technological Development and Innovations of the Republic of Serbia (337-00-19/2023-01/6). The work of K.Halaj is supported by the Ministry of Science, Technological Development and Innovations of the Republic of Serbia (the contract 451-03-65/2024-03/200128), while the work of B. Milošević and M. Veljović is supported by the Ministry of Science, Technological Development and Innovations of the Republic of Serbia (the contract the contract 451-03-66/2024-03/200104). The work of B. Milošević is also supported by the COST action CA21163 - Text, functional and other high-dimensional data in econometrics: New models, methods, applications (HiTEc).

Declarations

A Assumptions

Assumption A. Under H_0 , if δ denotes the true parameter value, then

$$\sqrt{n}(\hat{\delta} - \delta) = \frac{1}{\sqrt{n}} \sum_{i=1}^n L_1(\theta_{\varepsilon_j}; \delta) + r_\delta,$$

with $r_\delta = o_p(1)$, $\mathbb{E}\{L_1(\theta; \delta)\} = 0$ and $\mathbb{E}\{L_1(\theta; \delta)^2\} < \infty$.

Assumption B. Under H_0 , if $u = (\theta_0, \theta_1, r)^T$ denotes the true parameter value, then

$$\sqrt{n}(\hat{u} - u) = \frac{1}{\sqrt{n}} \sum_{i=1}^n L_2(\theta_{\varepsilon_j}; u) + r_u,$$

with $r_u = o_p(1)$, $\mathbb{E}\{L_2(\theta; u)\} = \mathbf{0}$, $\mathbb{E}\{L_2(\theta; u)L_2(\theta; u)^\top\} < \infty$, and $L_2(\cdot; \cdot)$ is not identically equal to $\mathbf{0}$.

Assumption C. The weight function ω is nonnegative and

$$\sum_{t=0}^{\infty} t^2 \omega(t) < \infty.$$

B Proof of Theorem 1

Proof 1 We can represent the test statistics as

$$T_n = n \cdot \sum_{t=0}^{\infty} \left| \widehat{\varphi}_n(t) - \varphi(t, \widehat{\delta}) \right|^2 \omega(t) = \sum_{t=0}^{\infty} \left| I_n^{(1)}(t) + I_n^{(2)}(t) \right|^2 \omega(t),$$

where

$$I_n^{(1)}(t) = \frac{1}{\sqrt{n}} \sum_{j=1}^n (\cos(t\theta_{\varepsilon_j}) + i \sin(t\theta_{\varepsilon_j}) - \delta^t), \quad I_n^{(2)}(t) = \sqrt{n} (\delta^t - \widehat{\delta}^t).$$

The main idea is to decompose $I_n^{(1)}(t)$ and $I_n^{(2)}(t)$ into sums of independent and identically distributed (i.i.d.) random variables and negligible remainders. This approach allows us to apply the central limit theorem (CLT) in Hilbert space. We start with the expansion of $I_n^{(1)}(t)$.

We have

$$\begin{aligned} I_n^{(1)}(t) &= \frac{1}{\sqrt{n}} \sum_{j=1}^n (\cos(t\theta_{\varepsilon_j}) + i \sin(t\theta_{\varepsilon_j}) - \delta^t) \\ &+ \frac{t}{\sqrt{n}} \sum_{j=1}^n (\theta_{\widehat{\varepsilon}_j} - \theta_{\varepsilon_j}) (i \cos(t\theta_{\varepsilon_j}) - \sin(t\theta_{\varepsilon_j})) + \frac{1}{\sqrt{n}} \sum_{j=1}^n (R_{1j}(t) + iR_{2j}(t)), \end{aligned}$$

where, for some $\gamma \in [0, 1]$,

$$\begin{aligned} R_{1j}(t) &= -\frac{1}{2} \cos(\gamma t \theta_{\widehat{\varepsilon}_j} + (1 - \gamma)t \theta_{\varepsilon_j}) t^2 (\theta_{\widehat{\varepsilon}_j} - \theta_{\varepsilon_j})^2, \\ R_{2j}(t) &= -\frac{1}{2} \sin(\gamma t \theta_{\widehat{\varepsilon}_j} + (1 - \gamma)t \theta_{\varepsilon_j}) t^2 (\theta_{\widehat{\varepsilon}_j} - \theta_{\varepsilon_j})^2. \end{aligned}$$

Let $\theta_0^{(0)}, \theta_1^{(0)}, r^{(0)}$ be null model parameters, $u_0 = (\theta_0^{(0)}, \theta_1^{(0)}, r^{(0)})^T$ and $\theta_y^{(0)} = \text{Arg} \left(\beta_0^{(0)} \frac{x + \beta_1^{(0)}}{1 + \beta_1^{(0)} x} \varepsilon \right)$, where $\beta_0^{(0)} = e^{i\theta_0^{(0)}}$ and $\beta_1^{(0)} = r^{(0)} e^{i\theta_1^{(0)}}$. Defining

$$\begin{aligned} A_j(\theta_0, \theta_1, r) &= \frac{r^2 \cos(\theta_0 + 2\theta_1 - \theta_{x_j} - \theta_y^{(0)}) + 2r \cos(\theta_0 + \theta_1 - \theta_y^{(0)})}{r^2 + 2r \cos(\theta_1 - \theta_{x_j}) + 1} \\ &+ \frac{\cos(\theta_0 + \theta_{x_j} - \theta_y^{(0)})}{r^2 + 2r \cos(\theta_1 - \theta_{x_j}) + 1}, \\ B_j(\theta_0, \theta_1, r) &= -\frac{r^2 \sin(\theta_0 + 2\theta_1 - \theta_{x_j} - \theta_y^{(0)}) + 2r \sin(\theta_0 + \theta_1 - \theta_y^{(0)})}{r^2 + 2r \cos(\theta_1 - \theta_{x_j}) + 1} \\ &- \frac{\sin(\theta_0 + \theta_{x_j} - \theta_y^{(0)})}{r^2 + 2r \cos(\theta_1 - \theta_{x_j}) + 1}, \end{aligned}$$

we have $\theta_{\widehat{\varepsilon}_j} = \text{atan2}(B_j(\widehat{u}), A_j(\widehat{u}))$ and $\theta_{\varepsilon_j} = \text{atan2}(B_j(u_0), A_j(u_0))$. Further, a Taylor expansion yields

$$\theta_{\widehat{\varepsilon}_j} = \theta_{\varepsilon_j} + \nabla(\text{atan2})(B_j(u), A_j(u)) \nabla(B_j, A_j)(u) \Big|_{u=u_0^*} (\widehat{u} - u_0) + r_j, \quad (8)$$

where

$$\begin{aligned} r_j &= \frac{1}{2} (\widehat{u} - u_0)^T \nabla^2(\text{atan2}(B_j(u), A_j(u)) \Big|_{u=u_0^*} (\widehat{u} - u_0) \\ &= (\widehat{u} - u_0)^T M_j(u_0^*) (\widehat{u} - u_0) = O_p(1/n), \end{aligned}$$

∇^2 represents the Hessian matrix, and u_0^* is between \widehat{u} and u_0 . The explicit expression for $M_j(u_0^*)$ is cumbersome, so we do not show it here. However, using the following expressions and further tedious calculations, it can be shown that it is bounded. Expressions for $\nabla(\text{atan2}(B_j(u), A_j(u)))$ and $\nabla(B_j, A_j)(u)$ in (8) are given by

$$\nabla(\text{atan2})(B_j(u), A_j(u)) = \left(\frac{\partial \text{atan2}}{\partial B} (B_j(u), A_j(u)) \quad \frac{\partial \text{atan2}}{\partial A} (B_j(u), A_j(u)) \right) \text{ and}$$

$$\nabla(B_j, A_j)(u) = \begin{pmatrix} \frac{\partial B_j}{\partial \theta_0}(u) & \frac{\partial B_j}{\partial \theta_1}(u) & \frac{\partial B_j}{\partial r}(u) \\ \frac{\partial A_j}{\partial \theta_0}(u) & \frac{\partial A_j}{\partial \theta_1}(u) & \frac{\partial A_j}{\partial r}(u) \end{pmatrix}$$

where

$$\begin{aligned} \frac{\partial B_j}{\partial \theta_0}(u) &= -\frac{r^2 \cos(\theta_0 + 2\theta_1 - \theta_{x_j} - \theta_y^{(0)}) + 2r \cos(\theta_0 + \theta_1 - \theta_y^{(0)}) + \cos(\theta_0 + \theta_{x_j} - \theta_y^{(0)})}{r^2 + 2r \cos(\theta_1 - \theta_{x_j}) + 1}, \\ \frac{\partial B_j}{\partial \theta_1}(u) &= -\frac{2r^2 \cos(\theta_0 + 2\theta_1 - \theta_{x_j} - \theta_y^{(0)}) + 2r \cos(\theta_0 + \theta_1 - \theta_y^{(0)})}{r^2 + 2r \cos(\theta_1 - \theta_{x_j}) + 1} \\ &\quad - \frac{2r \sin(\theta_1 - \theta_{x_j}) \left(r^2 \sin(\theta_0 + 2\theta_1 - \theta_{x_j} - \theta_y^{(0)}) + 2r \sin(\theta_0 + \theta_1 - \theta_y^{(0)}) \right)}{(r^2 + 2r \cos(\theta_1 - \theta_{x_j}) + 1)^2} \\ &\quad - \frac{2r \sin(\theta_1 - \theta_{x_j}) \left(\sin(\theta_0 + \theta_{x_j} - \theta_y^{(0)}) \right)}{(r^2 + 2r \cos(\theta_1 - \theta_{x_j}) + 1)^2}, \\ \frac{\partial B_j}{\partial r}(u) &= \frac{(2r + 2 \cos(\theta_1 - \theta_{x_j})) \left(r^2 \sin(\theta_0 + 2\theta_1 - \theta_{x_j} - \theta_y^{(0)}) + 2r \sin(\theta_0 + \theta_1 - \theta_y^{(0)}) \right)}{(r^2 + 2r \cos(\theta_1 - \theta_{x_j}) + 1)^2} \\ &\quad + \frac{(2r + 2 \cos(\theta_1 - \theta_{x_j})) \left(\sin(\theta_0 + \theta_{x_j} - \theta_y^{(0)}) \right)}{(r^2 + 2r \cos(\theta_1 - \theta_{x_j}) + 1)^2} \\ &\quad - \frac{2r \sin(\theta_0 + 2\theta_1 - \theta_{x_j} - \theta_y^{(0)}) + 2 \sin(\theta_0 + \theta_1 - \theta_y^{(0)})}{r^2 + 2r \cos(\theta_1 - \theta_{x_j}) + 1}, \\ \frac{\partial A_j}{\partial \theta_0}(u) &= \frac{r^2 (-\sin(\theta_0 + 2\theta_1 - \theta_{x_j} - \theta_y^{(0)})) - 2r \sin(\theta_0 + \theta_1 - \theta_y^{(0)}) - \sin(\theta_0 + \theta_{x_j} - \theta_y^{(0)})}{r^2 + 2r \cos(\theta_1 - \theta_{x_j}) + 1}, \\ \frac{\partial A_j}{\partial \theta_1}(u) &= \frac{2r \sin(\theta_1 - \theta_{x_j}) \left(r^2 \cos(\theta_0 + 2\theta_1 - \theta_{x_j} - \theta_y^{(0)}) + 2r \cos(\theta_0 + \theta_1 - \theta_y^{(0)}) \right)}{(r^2 + 2r \cos(\theta_1 - \theta_{x_j}) + 1)^2} \\ &\quad + \frac{2r \sin(\theta_1 - \theta_{x_j}) \left(\cos(\theta_0 + \theta_{x_j} - \theta_y^{(0)}) \right)}{(r^2 + 2r \cos(\theta_1 - \theta_{x_j}) + 1)^2} \\ &\quad + \frac{-2r^2 \sin(\theta_0 + 2\theta_1 - \theta_{x_j} - \theta_y^{(0)}) - 2r \sin(\theta_0 + \theta_1 - \theta_y^{(0)})}{r^2 + 2r \cos(\theta_1 - \theta_{x_j}) + 1}, \\ \frac{\partial A_j}{\partial r}(u) &= \frac{2r \cos(\theta_0 + 2\theta_1 - \theta_{x_j} - \theta_y^{(0)}) + 2 \cos(\theta_0 + \theta_1 - \theta_y^{(0)})}{r^2 + 2r \cos(\theta_1 - \theta_{x_j}) + 1} \\ &\quad - \frac{(2r + 2 \cos(\theta_1 - \theta_{x_j})) \left(r^2 \cos(\theta_0 + 2\theta_1 - \theta_{x_j} - \theta_y^{(0)}) + 2r \cos(\theta_0 + \theta_1 - \theta_y^{(0)}) \right)}{(r^2 + 2r \cos(\theta_1 - \theta_{x_j}) + 1)^2} \\ &\quad - \frac{(2r + 2 \cos(\theta_1 - \theta_{x_j})) \left(\cos(\theta_0 + \theta_{x_j} - \theta_y^{(0)}) \right)}{(r^2 + 2r \cos(\theta_1 - \theta_{x_j}) + 1)^2}. \end{aligned}$$

Further, we obtain

$$\begin{aligned} \left| \frac{1}{\sqrt{n}} \sum_{j=1}^n R_{1j}(t) \right| &\leq \frac{1}{2n^{\frac{3}{2}}} t^2 \sum_{j=1}^n \left| \sqrt{n}(\theta_{\varepsilon_j} - \theta_{\varepsilon_j}) \right|^2 \\ &= \frac{1}{2n^{\frac{3}{2}}} \sum_{j=1}^n t^2 \left| \left(\nabla(\text{atan2})(B_j(u), A_j(u)) \nabla(B_j, A_j)(u) \right) \Big|_{u=u_0} \sqrt{n}(\hat{u} - u_0) + \sqrt{n}r_j \right|^2 \end{aligned}$$

$$\begin{aligned} &\leq \frac{1}{2n^{\frac{3}{2}}} \sum_{j=1}^n t^2 \left\| \left(\nabla(\operatorname{atan2})(B_j(u), A_j(u)) \nabla(B_j, A_j)(u) \right) \Big|_{u=u_0} \right\|^2 \|\sqrt{n}(\hat{u} - u_0)\|^2 \\ &+ \frac{1}{2\sqrt{n}} \sum_{j=1}^n t^2 \|r_j\|^2 = t^2 O_p\left(\frac{1}{\sqrt{n}}\right), \end{aligned}$$

and, similarly, $\left| \frac{1}{\sqrt{n}} \sum_{j=1}^n R_{2j}(t) \right| \leq t^2 O_p(1/\sqrt{n})$. Applying the delta method yields

$$\sqrt{n}(\hat{\delta}^t - \delta^t) = \sqrt{nt} \delta^{t-1} (\hat{\delta} - \delta) + o_p(1) = t \delta^{t-1} \left(\frac{1}{\sqrt{n}} \sum_{i=1}^n L_1(\theta_{\varepsilon_j}; \delta) + r_\delta \right) + o_p(1).$$

By assumptions A and C, $\|t \delta^{t-1} r_\delta\|_w = o_p(1)$. Combining the results, we obtain

$$\begin{aligned} I_n^{(1)}(t) + I_n^{(2)}(t) &= \frac{1}{\sqrt{n}} \sum_{j=1}^n \left(\cos(t\theta_{\varepsilon_j}) + i \sin(t\theta_{\varepsilon_j}) - \delta^t \right. \\ &\quad \left. + t(\theta_{\varepsilon_j} - \theta_{\varepsilon_j}) (i \cos(t\theta_{\varepsilon_j}) - \sin(t\theta_{\varepsilon_j})) + t \delta^{t-1} L_1(\theta_{\varepsilon_j}; \delta) \right) + o_p(1) \\ &= \frac{1}{\sqrt{n}} \sum_{j=1}^n \left(\cos(t\theta_{\varepsilon_j}) + i \sin(t\theta_{\varepsilon_j}) - \delta^t \right. \\ &\quad \left. + it \left(\nabla(\operatorname{atan2})(B_j(u), A_j(u)) \nabla(B_j, A_j)(u) \right) \Big|_{u=u_0} \frac{1}{n} \sum_{k=1}^n L_2(\theta_{\varepsilon_k}; u_0) \cos(t\theta_{\varepsilon_j}) \right. \\ &\quad \left. - t \left(\nabla(\operatorname{atan2})(B_j(u), A_j(u)) \nabla(B_j, A_j)(u) \right) \Big|_{u=u_0} \frac{1}{n} \sum_{k=1}^n L_2(\theta_{\varepsilon_k}; u_0) \sin(t\theta_{\varepsilon_j}) \right. \\ &\quad \left. + t \delta^{t-1} L_1(\theta_{\varepsilon_j}; \delta) \right) + r_{tot}(t), \end{aligned}$$

where $r_{tot}(t)$ is the sum of the remainders that appear in the approximations used so far, satisfying

$$\left| \frac{1}{\sqrt{n}} \sum_{j=1}^n r_{tot,j}(t) \right| \leq t^2 o_p(1).$$

Let $C(\theta_{\varepsilon_j}) = \left(\nabla(\operatorname{atan2})(B_j(u), A_j(u)) \nabla(B_j, A_j)(u) \right) \Big|_{u=u_0}$ and

$$\Phi^{(1)}(\theta_{\varepsilon_j}, \theta_{\varepsilon_k}; t) = \frac{1}{2} (C(\theta_{\varepsilon_k}) L_2(\theta_{\varepsilon_j}; u_0) \cos(t\theta_{\varepsilon_k}) + C(\theta_{\varepsilon_j}) L_2(\theta_{\varepsilon_k}; u_0) \cos(t\theta_{\varepsilon_j})),$$

$$\Phi^{(2)}(\theta_{\varepsilon_j}, \theta_{\varepsilon_k}; t) = \frac{1}{2} (C(\theta_{\varepsilon_k}) L_2(\theta_{\varepsilon_j}; u_0) \sin(t\theta_{\varepsilon_k}) + C(\theta_{\varepsilon_j}) L_2(\theta_{\varepsilon_k}; u_0) \sin(t\theta_{\varepsilon_j})).$$

Then, if we denote $V_n^{(1)}(t) = \frac{1}{n^2} \sum_{j=1}^n \sum_{k=1}^n \Phi^{(1)}(\theta_{\varepsilon_j}, \theta_{\varepsilon_k}; t)$ and $V_n^{(2)}(t) = \frac{1}{n^2} \sum_{j=1}^n \sum_{k=1}^n \Phi^{(2)}(\theta_{\varepsilon_j}, \theta_{\varepsilon_k}; t)$, using Hoeffding's theorem for the asymptotic distribution of V-statistics, we get that $\sqrt{n} V_n^{(i)}(t) \xrightarrow{L} \mathcal{N}(0, 4\sigma_{(i)}^2(t))$, where $\sigma_{(i)}^2(t) = E(\Phi_1^{(i)}(\theta_\varepsilon; t))^2$, $i = 1, 2$, and

$$\Phi_1^{(1)}(x; t) = E\Phi^{(1)}(x, \theta_\varepsilon; t) = \frac{1}{2} E\left(C(\theta_\varepsilon) L_2(x; u_0) \cos(t\theta_\varepsilon) \right),$$

$$\Phi_1^{(2)}(x; t) = E\Phi^{(2)}(x, \theta_\varepsilon; t) = \frac{1}{2} E\left(C(\theta_\varepsilon) L_2(x; u_0) \sin(t\theta_\varepsilon) \right)$$

are the first projections of kernels $\Phi^{(1)}$ and $\Phi^{(2)}$, respectively. It can be numerically shown, taking into account that $L_2(\cdot, u_0) \neq \mathbf{0}$, that these projections are nonconstant functions. Then, we have

$$I_n^{(1)}(t) + I_n^{(2)}(t) = \frac{1}{\sqrt{n}} \sum_{j=1}^n \left(\cos(t\theta_{\varepsilon_j}) + i \sin(t\theta_{\varepsilon_j}) - \delta^t + t \delta^{t-1} L_1(\theta_{\varepsilon_j}; \delta) \right)$$

$$\begin{aligned}
& + it\sqrt{n}V_n^{(1)}(t) - t\sqrt{n}V_n^{(2)}(t) + r_{tot}(t) \\
& = \frac{1}{\sqrt{n}} \sum_{j=1}^n \left(\cos(t\theta_{\varepsilon_j}) + i \sin(t\theta_{\varepsilon_j}) - \delta^t + t\delta^{t-1}L_1(\theta_{\varepsilon_j}; \delta) \right. \\
& \quad \left. + 2it\Phi_1^{(1)}(\theta_{\varepsilon_j}; t) - 2t\Phi_1^{(2)}(\theta_{\varepsilon_j}; t) \right) + R'(t) \\
& = \frac{1}{\sqrt{n}} \sum_{j=1}^n \Gamma(t, \theta_{\varepsilon_j}; u_0, \delta) + R'(t).
\end{aligned}$$

From the bound for $r_{tot}(t)$ and the Hoeffding approximation of the V-statistic, it follows that $|R'(t)| \leq o_p(1)t^2$. Furthermore, due to the fact that L_1 and L_2 have expectation 0, it can be seen that $E\{\Gamma(t, \theta_{\varepsilon_1}; u_0, \delta)\} = 0$. Finally, applying the central limit theorem in Hilbert spaces (see e.g. [2]), we obtain that the limiting process is a centered Gaussian with covariance kernel

$$K_G(s, t) = \mathbb{E}\{\Gamma(t, \theta_{\varepsilon}; u_0, \delta)\bar{\Gamma}(s, \theta_{\varepsilon}; u_0, \delta)\}, \quad (9)$$

where $\Gamma(t, \theta_{\varepsilon}; u_0, \delta) = \cos(t\theta_{\varepsilon}) + i \sin(t\theta_{\varepsilon}) - \delta^t + t\delta^{t-1}L_1(\theta_{\varepsilon}; \delta) + 2it\Phi_1^{(1)}(\theta_{\varepsilon}; t) - 2t\Phi_1^{(2)}(\theta_{\varepsilon}; t)$. The statement of Theorem 1 is now a direct consequence of the continuous mapping theorem.

C Circular densities of the alternative distributions

- wrapped normal distribution $\mathcal{WN}(\mu, \rho)$

$$f(\theta) = \frac{1}{2\pi} \left(1 + 2 \sum_{k=1}^{\infty} \rho^{k^2} \cos k(\theta - \mu) \right), \quad 0 \leq \theta, \mu < 2\pi, \quad 0 < \rho < 1.$$

- von Mises distribution $\mathcal{VM}(\mu, k)$

$$f(\theta) = \frac{1}{2\pi I_0(k)} e^{k \cos(\theta - \mu)}, \quad 0 \leq \theta, \mu < 2\pi, \quad k > 0,$$

where $I_0(k)$ is the modified Bessel function of the first kind.

- cardioid distribution $\mathcal{Ca}(\mu, \rho)$

$$f(\theta) = \frac{1}{2\pi} (1 + 2\rho \cos(\theta - \mu)), \quad 0 \leq \theta, \mu < 2\pi, \quad |\rho| < \frac{1}{2},$$

- Cartwright's power-of-cosine distribution $\mathcal{CW}(\mu, \zeta)$

$$f(\theta) = \frac{2^{\frac{1}{\zeta}-1} \Gamma^2\left(\frac{1}{\zeta} + 1\right) (1 + \cos(\theta - \mu))^{1/\zeta}}{\pi \Gamma\left(\frac{2}{\zeta} + 1\right)}, \quad 0 \leq \theta, \mu < 2\pi, \quad \zeta > 0,$$

where $\Gamma(\cdot)$ is the gamma function.

- Jones-Pewsey distribution $\mathcal{JP}(\mu, \kappa, \psi)$

$$f(\theta) = \frac{\cosh(\kappa\psi) + \sinh(\kappa\psi) \cos(\theta - \mu)^{\frac{1}{\psi}}}{2\pi P_{\frac{1}{\psi}}(\cosh(\kappa\psi))}, \quad 0 \leq \theta, \mu < 2\pi, \quad \kappa \geq 0, \quad \psi \in \mathbb{R},$$

where $P_{\frac{1}{\psi}}(\cdot)$ is the associated Legendre function of the first kind with degree $\frac{1}{\psi}$ and order 0.

- Batschelet distribution $\mathcal{Ba}(\mu, \kappa, \nu)$

$$f(\theta) = \frac{1}{B_0(\kappa, \nu)} e^{\kappa \cos((\theta - \mu) + \nu \sin(\theta - \mu))}, \quad 0 \leq \theta, \mu < 2\pi, \quad \kappa \geq 0, \quad -1 \leq \nu \leq 1,$$

where

$$B_p(\kappa, \nu) = \int_0^{2\pi} \cos(p\theta) e^{\kappa \cos(\theta + \nu \sin \theta)} d\theta, \quad p = 0, 1, \dots$$

D Classical bootstrap algorithm

1. For fixed x_1, x_2, \dots, x_n and y_1, y_2, \dots, y_n compute the estimator $\hat{v}_n := \hat{v}_n(x_1, x_2, \dots, x_n; y_1, y_2, \dots, y_n)$ of the parameter vector $v = (\theta_0, \theta_1, r, \delta)$.
2. Calculate the residuals $\hat{\theta}_\varepsilon$ of the proposed regression model, using $\hat{y} = \hat{\beta}_0 \frac{x + \hat{\beta}_1}{1 + \hat{\beta}_1 x}$.
3. Compute the test statistic of interest, say $S_n = S_n(\hat{\theta}_{\varepsilon_1}, \hat{\theta}_{\varepsilon_2}, \dots, \hat{\theta}_{\varepsilon_n}; \hat{v}_n)$.
4. Repeat the following steps for each $i \in \{1, \dots, B\}$:
 - a) Generate a bootstrap sample $y_1^*, y_2^*, \dots, y_n^*$, where $y_j^* = \hat{\beta}_0 \frac{x + \hat{\beta}_1}{1 + \hat{\beta}_1 x} \varepsilon_j^*$ and $\varepsilon_j^* \sim WC(\hat{\delta})$.
 - b) On the basis of (y_1^*, \dots, y_n^*) , obtain a bootstrap estimate \hat{v}_n^* of v .
 - c) Calculate the residuals $\hat{\theta}_\varepsilon^*$ of the proposed regression model, using $\hat{y}^* = \hat{\beta}_0^* \frac{x + \hat{\beta}_1^*}{1 + \hat{\beta}_1^* x}$.
 - d) Compute the value of the bootstrap test statistic $S_n^{*(i)} = S_n(\hat{\theta}_{\varepsilon_1}^*, \hat{\theta}_{\varepsilon_2}^*, \dots, \hat{\theta}_{\varepsilon_n}^*; \hat{v}_n^*)$.
5. Reject the null hypothesis if $S_n \geq c_\alpha$, where c_α denotes the $(1 - \alpha)\%$ quantile of the empirical distribution of the bootstrap test statistics $(S_n^{*(1)}, \dots, S_n^{*(B)})$.

E Warp-speed bootstrap algorithm

1. For fixed covariates x_1, x_2, \dots, x_n , simulate a sequence $\varepsilon_1, \varepsilon_2, \dots, \varepsilon_n \sim F_1$, where F_1 denotes one of the alternative distributions defined above, and the corresponding y_1, y_2, \dots, y_n .
2. Compute the estimator $\hat{v}_n := \hat{v}_n(x_1, x_2, \dots, x_n; y_1, y_2, \dots, y_n)$ of the parameter vector $v = (\theta_0, \theta_1, r, \delta)$.
3. Calculate the residuals $\hat{\theta}_\varepsilon$ of the proposed regression model, using $y_{fit} = \hat{\beta}_0 \frac{x + \hat{\beta}_1}{1 + \hat{\beta}_1 x}$.
4. Compute the test statistic of interest, say $S_n = S_n(\hat{\theta}_{\varepsilon_1}, \hat{\theta}_{\varepsilon_2}, \dots, \hat{\theta}_{\varepsilon_n}; \hat{v}_n)$.
5. Generate a bootstrap sample $y_1^*, y_2^*, \dots, y_n^*$, where $y_j^* = \hat{\beta}_0 \frac{x + \hat{\beta}_1}{1 + \hat{\beta}_1 x} \varepsilon_j^*$ and $\varepsilon_j^* \sim WC(\hat{\delta})$.
6. On the basis of (y_1^*, \dots, y_n^*) , obtain a bootstrap estimate \hat{v}_n^* of v .
7. Calculate the residuals $\hat{\theta}_\varepsilon^*$ of the proposed regression model, using $\hat{y}^* = \hat{\beta}_0^* \frac{x + \hat{\beta}_1^*}{1 + \hat{\beta}_1^* x}$.
8. Compute the value of the bootstrap test statistic $S_n^* = S_n(\hat{\theta}_{\varepsilon_1}^*, \hat{\theta}_{\varepsilon_2}^*, \dots, \hat{\theta}_{\varepsilon_n}^*; \hat{v}_n^*)$.
9. Repeat the previous steps B times and thereby produce two sequences of test statistics: $\{S_n^{(1)}, S_n^{(2)}, \dots, S_n^{(B)}\}$ and $\{S_n^{*(1)}, S_n^{*(2)}, \dots, S_n^{*(B)}\}$.
10. Reject the null hypothesis for the j -th sample ($j = 1, \dots, B$), if $S_n^{(j)} \geq c_\alpha$, where c_α denotes the $(1 - \alpha)\%$ quantile of the empirical distribution of the bootstrap test statistics $(S_n^{*(1)}, \dots, S_n^{*(B)})$.

References

- [1] C. Agostinelli and U. Lund. *R package circular: Circular Statistics (version 0.5-0)*, 2023.
- [2] D. Bosq. *Linear processes in function spaces: theory and applications*, volume 149. Springer Science & Business Media, Paris, 2000.
- [3] T. D. Downs. Rotational angular correlation. *Biorhythm and Human Reproduction*, pages 97–104, 1974.
- [4] B. Ebner, M. D. Jiménez-Gamero, and B. Milošević. Eigenvalues approximation of integral covariance operators with applications to weighted l^2 statistics. *arXiv preprint arXiv:2408.08064*, 2024.
- [5] R. Giacomini, D. N. Politis, and H. White. A warp-speed method for conducting monte carlo experiments involving bootstrap estimators. *Econometric Theory*, 29(3):567–589, 2013.
- [6] W. González-Manteiga and R. M. Crujeiras. An updated review of goodness-of-fit tests for regression models. *Test*, 22:361–411, 2013.

- [7] F. H. Hodel and J. R. Fieberg. Cylcop: An R package for circular-linear copulae with angular symmetry. *bioRxiv*, 2021.
- [8] R. V. Hogg, J. W. McKean, and A. T. Craig. *Introduction to mathematical statistics*. Pearson, United States of America, 2019.
- [9] R. S. Jammalamadaka, M. D. Jiménez Gamero, and S. G. Meintanis. A class of goodness-of-fit tests for circular distributions based on trigonometric moments. *SORT*, 43, 317-336., 2019.
- [10] S. R. Jammalamadaka and Y. R. Sarma. A correlation coefficient for angular variables. *Statistical theory and data analysis II*, pages 349–364, 1988.
- [11] R. A. Johnson and T. Wehrly. Measures and models for angular correlation and angular–linear correlation. *Journal of the Royal Statistical Society Series B: Statistical Methodology*, 39(2):222–229, 1977.
- [12] S. Kato, K. Shimizu, and G. S. Shieh. A circular–circular regression model. *Statistica Sinica*, pages 633–645, 2008.
- [13] D. Liu, S. D. Peddada, L. Li, and C. R. Weinberg. Phase analysis of circadian-related genes in two tissues. *BMC bioinformatics*, 7:1–10, 2006.
- [14] S. G. Meintanis, M. D. J. Gamero, and V. Alba-Fernández. A class of goodness-of-fit tests based on transformation. *Communications in Statistics-Theory and Methods*, 43(8):1708–1735, 2014.
- [15] A. Pewsey and E. García-Portugués. Recent advances in directional statistics. *Test*, 30(1):1–58, 2021.
- [16] R Core Team. *R: A Language and Environment for Statistical Computing*. R Foundation for Statistical Computing, Vienna, Austria, 2024.